Available online at www.sciencedirect.com
SCIENCE DIRECT®
Bioorganic & Medicinal Chemistry Letters 15 (2005) 4699–4702
Bioorganic & Medicinal Chemistry Letters

Synthesis of 4-(5-[^{18}F]fluoromethyl-3-phenylisoxazol-4-yl)-benzenesulfonamide, a new [^{18}F]fluorinated analogue of valdecoxib, as a potential radiotracer for imaging cyclooxygenase-2 with positron emission tomography

Tatsushi Toyokuni,[a,*] J. S. Dileep Kumar,[a] Joseph C. Walsh,[a] Alan Shapiro,[a] John J. Talley,[b] Michael E. Phelps,[a] Harvey R. Herschman,[a] Jorge R. Barrio[a] and Nagichettiar Satyamurthy[a]

[a]*Crump Institute for Molecular Imaging and LA Tech Center, Department of Molecular and Medical Pharmacology, David Geffen School of Medicine at University of California, Los Angeles, CA 90095, USA*
[b]*Searle Research and Development, St. Louis, MO 63198, USA*

Received 18 June 2005; revised 27 July 2005; accepted 27 July 2005
Available online 8 September 2005

Abstract—Fluoroalkyl and fluoroaryl analogues of valdecoxib were found to possess potent inhibitory activities against cyclooxygenase-2 comparable to that of the parent valdecoxib. Among them, the fluoromethyl analogue was chosen for ^{18}F-labeling. Thus, 4-(5-[^{18}F]fluoromethyl-3-phenylisoxazol-4-yl)benzenesulfonamide (~2000 Ci/mmol at end of synthesis) was synthesized by [^{18}F]fluoride-ion displacement of the corresponding tosylate in ~40% decay-corrected radiochemical yield within ~120 min from end of bombardment.

Cyclooxygenase (COX) is the enzyme that catalyzes the first step in the biotransformation of arachidonic acid to prostanoids.[1] COX exists as two distinct isoforms, of which COX-1 is constitutively expressed in healthy tissues mediating physiological responses, while COX-2 is the inducible form responsible for the synthesis of prostanoids involved in acute and chronic inflammatory states. Inflammation is a common biological process shared by many diseases. Indeed, elevated expression of COX-2 has been implicated in many pathological events, including rheumatoid arthritis, cancer, heart disease, stroke, and neurodegenerative disorders.[1b,c,2] However, COX-2 is also found constitutively in some tissues where it is considered to play a physiologically important role.[1b,c]

The therapeutic effect of classical non-steroidal anti-inflammatory drugs (NSAIDs) is attributed to the inhibition of COX-2, whereas the undesired side effects arise from the disruption of COX-1. Since the discovery of COX-2 in 1991,[1a] a rapid progress has been made in the development of COX-2-selective inhibitors.[3] In 1999, celecoxib (Celebrex) and rofecoxib (Vioxx) were introduced to the market as non-ulcerogenic anti-inflammatory drugs. Subsequently, in 2001, a second generation inhibitor valdecoxib (Bextra) received the US Food and Drug Administration (FDA) approval. However, clinical trial studies with these drugs have raised concerns about their potential cardiovascular hazards.[4] As a result, Vioxx and Bextra have recently been withdrawn from the worldwide market and a black-box warning is being required for Celebrex.[5]

To fully understand the role of COX-2 both in health and disease, it would be of great benefit if we could monitor 'real-time' COX-2 expression in vivo, non-invasively and repeatedly over time.[6] COX-2-selective inhibitors labeled with short-lived positron emitters are therefore attractive molecules that could be used to image COX-2 in living subjects with positron emission tomography (PET), which is a powerful non-invasive, in vivo molecular imaging technique currently available for biomedi-

Keywords: PET; Radiotracer; Fluorine-18; COX-2; Inhibitor; Valdecoxib.
* Corresponding author. E-mail: ttoyokuni@mednet.ucla.edu

0960-894X/$ - see front matter © 2005 Elsevier Ltd. All rights reserved.
doi:10.1016/j.bmcl.2005.07.065

cal use.[7] The [^{18}F]fluorinated or [^{11}C]methylated analogues of celecoxib,[8,9] rofecoxib,[10] and their prototype DuP-697[11] have recently been synthesized. Herein, we report the synthesis of a new [^{18}F]fluorinated analogue of valdecoxib **1-^{18}F** (Fig. 1) as a potential PET imaging probe for COX-2.[12]

Being bioisosteric with hydrogen, albeit having high electronegativity,[13] ^{18}F is often used to replace hydrogen of otherwise non-fluorinated molecules with minimum effects on biomolecular interactions. Non-radioactive fluorinated analogues of valdecoxib were first synthesized and evaluated for their COX-2 inhibitory activities using human recombinant COX-1 and COX-2 enzymes,[14] and/or endotoxin-treated RAW 264.7 macrophages.[15] The fluoroalkyl analogues **1**[16] and **2**[17] were synthesized by direct fluorination of the corresponding hydroxy analogues **5**[18] and **6**,[19] respectively, with DAST (Scheme 1). The fluoroaryl analogues **3** and **4** were synthesized, as previously reported.[20] As shown in Table 1, the fluoroalkyl and fluoroaryl analogues were all potent COX-2 inhibitors. Moreover, the fluoromethyl analogue **1** showed an even higher COX-2-selectivity index than valdecoxib. Therefore, the radiosynthesis of the [^{18}F]fluoromethyl analogue **1-^{18}F** was investigated.

The [^{18}F]fluorination precursor **8**[21] was synthesized from **5** via selective protection of the sulfonamide group with a 4,4′-dimethoxytrityl (DMTr) group (→**7**[22]), followed by *O*-tosylation with Ts_2O (→**8**) (Scheme 2). Radiosynthesis of **1-^{18}F** was then effected by two consecutive reactions in one pot, namely [^{18}F]fluoride-for-tosylate substitution of **8**, followed by acidic deprotection.[23] The radioactive product was purified by HPLC and reconstituted in EtOH (1 mL).[24] The specific activity was ~2000 Ci/mmol at end of synthesis (EOS). In a typical radiosynthesis, starting from ~500 mCi of [^{18}F]fluoride, ~80 mCi of chemically and radiochemically pure **1-^{18}F** was obtained in an injection-ready form within 120 min after end of bombardment (EOB). The decay-corrected radiochemical yield was ~40%. It was observed that **1-^{18}F** experienced autoradiolysis in saline containing 10% EtOH (~5% de[^{18}F]fluorination after 6 h).[25] The autoradiolysis was however effectively suppressed in 100% EtOH (less than 0.5% de[^{18}F]fluorination after 6 h).

In vivo kinetics of **1-^{18}F** was preliminary evaluated using a normal mouse with microPET.[26] Rapid in vivo de[^{18}F]fluorination was evidenced by the conspicuous emergence of the bony skeleton, which is characteristic of [^{18}F]fluoride peripheral formation with rapid uptake in bone.[27] A similar peripheral metabolism was also observed in a vervet monkey, although it was somewhat slower.[28] It is likely that **1-^{18}F** is metabolized in vivo

Table 1. Inhibition of COX-2 by fluorinated analogues of valdecoxib

Compound	IC_{50} (μM)[a]		
	Enzyme assay[b]		Macrophage COX-2 assay[d]
	COX-2	S.I.[c]	
1	0.002	>50,000	0.002
2	0.008	>12,500	0.002
3	—[e]	—[e]	0.002
4	—[e]	—[e]	0.002
Valdecoxib	0.005	>20,000	—[e]

[a] Values are means of two experiments.
[b] Enzyme assays were performed against human recombinant COX-1 and COX-2 enzymes, as reported in Ref. 14.
[c] In vitro COX-2-selectivity index: COX-1 IC_{50}/COX-2 IC_{50}.
[d] Cell-based assays were performed for prostaglandin E_2 production as a function of COX-2 inhibition using endotoxin-treated murine RAW 264.7 macrophages, as reported in Ref. 15.
[e] Not determined.

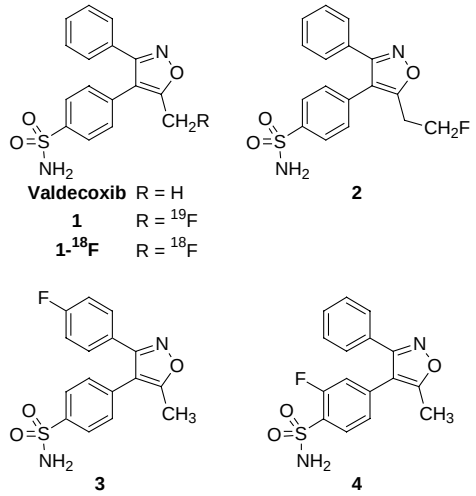

Figure 1. Valdecoxib and its [^{18}F/^{19}F]fluorinated analogues **1**–**4**.

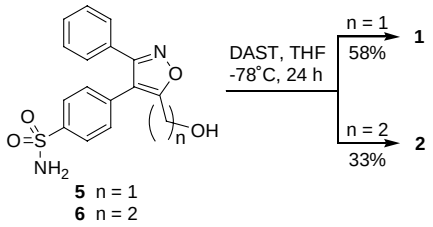

Scheme 1. Synthesis of non-radioactive fluoroalkylvaldecoxibs **1** and **2**.

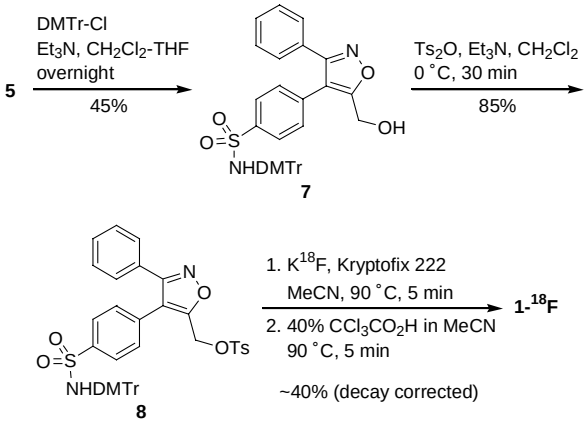

Scheme 2. Synthesis of [^{18}F]fluoromethylvaldecoxib (**1-^{18}F**).

similar to the parent valdecoxib, involving oxidative hydrogen abstraction at the methyl group presumably via the P450 enzyme-catalyzed oxidation process.[29] The [^{18}F]fluorohydroxymethyl group thus formed is chemically labile leading to spontaneous de[^{18}F]fluorination. It has been noted with drugs and other PET probes that the rate of peripheral metabolism increases in the order of mice > monkeys > humans.[30] Indeed, the metabolism of valdecoxib is reported to be rapid in rodents but significantly slower in humans.[29] Therefore, it would be expected that **1-^{18}F** would undergo a much slower metabolic de[^{18}F]fluorination in humans. The dosimetry data for a 70-kg adult were estimated from the residence times determined with the monkey whole-body biodistribution data using the MIRDOSE program (Table 2).[31] For a 10-mCi injection of **1-^{18}F**, the highest absorbed dose found in the urinary bladder wall was well below the dose limitation of 5 rad/mCi, warranting the safe use of **1-^{18}F** in human PET imaging studies.

In summary, the [^{18}F]fluoromethyl analogue of valdecoxib **1-^{18}F** has been synthesized. The rapid metabolic de[^{18}F]fluorination in mice hinders the determination of *in vivo* binding of **1-^{18}F** to COX-2 in experimental rodent models, limiting our ability to investigate **1-^{18}F** in detail. However, it should be mentioned that our preliminary human imaging results have shown the potential usefulness of **1-^{18}F** in human studies, because only minimum peripheral de[^{18}F]fluorination occurred after 60 min. In addition to PET imaging determination in humans, syntheses of radiofluorinated **2**–**4** are currently underway.

Table 2. Dosimetry estimation for **1-^{18}F** for a 70-kg adult

Target organ	Total dose (rad/mCi)
Adrenals	4.2×10^{-3}
Brain	3.1×10^{-5}
Breasts	1.1×10^{-2}
Gallbladder wall	8.5×10^{-3}
Lower large intestine wall	5.0×10^{-3}
Small intestine	6.4×10^{-3}
Stomach	2.6×10^{-3}
Upper large intestine wall	5.0×10^{-2}
Heart wall	1.8×10^{-2}
Kidneys	1.9×10^{-2}
Liver	3.4×10^{-2}
Lungs	2.3×10^{-3}
Muscle	1.8×10^{-3}
Ovaries	6.4×10^{-3}
Pancreas	3.8×10^{-3}
Red marrow	2.2×10^{-3}
Bone surfaces	1.2×10^{-3}
Skin	8.9×10^{-4}
Spleen	1.6×10^{-3}
Testes	2.8×10^{-3}
Thymus	2.0×10^{-3}
Thyroid	2.0×10^{-4}
Urinary bladder wall	1.4×10^{-1}
Uterus	1.0×10^{-2}
Total body	3.2×10^{-3}
Effective dose	1.3×10^{-2}

Acknowledgments

We thank the UCLA Biomedical Cyclotron staff, the UCLA microPET Imaging Facility staff, and the UCLA LA Tech Center Chemistry staff for their support. This research was supported in part by the Office of Science (BER), US Department of Energy, Cooperative Agreement No. DE-FC03-02ER63420, the National Institutes of Health (CA86306), and University of California Biotechnology STAR Grant 01-10184.

References and notes

1. (a) Herschman, H. R. *Biochim. Biophys. Acta* **1996**, *1299*, 125; (b) Turini, M. E.; DuBois, R. N. *Annu. Rev. Med.* **2002**, *53*, 35; (c) Simmons, D. L.; Botting, R. M.; Hla, T. *Pharmacol. Rev.* **2004**, *56*, 387.
2. Critical roles of COX-2 in the pathogenesis of Parkinson's disease and tumor angiogenesis have recently been identified. See: (a) Teismann, P.; Tieu, K.; Choi, D.; Wu, D.; Naini, A.; Hunot, S.; Vila, M.; Jackson-Lewis, V.; Przedborski, S. *Proc. Natl. Acad. Sci. U.S.A.* **2003**, *100*, 5473; (b) Hunot, S.; Vila, M.; Teismann, P.; Davis, R. J.; Hirsch, E. C.; Przedborski, S.; Rakic, P.; Flavell, R. A. *Proc. Natl. Acad. Sci. U.S.A.* **2004**, *101*, 665; (c) Chang, S.; Liu, C. H.; Conway, R.; Han, D. K.; Nithipatikom, K.; Trifan, O. C.; Lane, T. F.; Hla, T. *Proc. Natl. Acad. Sci. U.S.A.* **2004**, *101*, 591.
3. Talley, J. J. *Prog. Med. Chem.* **1999**, *36*, 201.
4. (a) Finckh, A.; Aronson, M. D. *Ann. Intern. Med.* **2005**, *142*, 212; (b) Dogné, J.-M.; Supuran, C. T.; Pratico, D. *J. Med. Chem.* **2005**, *48*, 2251.
5. A black-box warning is the most serious type of warning in prescription drug labeling.
6. Herschman, H. R.; Talley, J. J.; DuBois, R. *Mol. Imaging Biol.* **2003**, *5*, 286.
7. (a) Phelps, M. E. *Proc. Natl. Acad. Sci. U.S.A.* **2000**, *97*, 9226; (b) Fowler, J. S.; Wolf, A. P. *Acc. Chem. Res.* **1997**, *30*, 181.
8. (a) McCarthy, T. J.; Sheriff, A. U.; Graneto, M. J.; Talley, J. J.; Welch, M. J. *J. Nucl. Med.* **2002**, *43*, 117; (b) Kumar, J. S. D.; Prabhakaran, J.; Parsey, R. V.; Underwood, M. D.; Simpson, N. R.; Majo, V. J.; van Heertum, R.; Mann, J. J. Abstract of Papers, 50th Annual Meeting of the Society of Nuclear Medicine, New Orleans LA; Society of Nuclear medicine: VA, 2003; Abstract 1127; (c) Kumar, J. S. D.; Prabhakaran, J.; Underwood, M. D.; Parsey, R. V.; Arango, V.; Majo, V. J.; Simpson, N. R.; Arcement, J.; Cooper, A. R.; van Heertum, R. L.; Mann, J. J. Abstract of Papers, 226th National Meeting of the American Chemical Society, New York, NY; American Chemical Society: Washington, DC, 2003; Abstract MEDI 375.
9. The [^{123}I]iodinated analogue of celecoxib has also been synthesized for use with single photon emission computed tomography (SPECT). See: Kabalka, G. W.; Mereddy, A. R.; Schuller, H. M. *J. Labelled Compd. Radiopharm.* **2005**, *48*, 295.
10. Wüst, F. R.; Höhne, A.; Metz, P. *Org. Biomol. Chem.* **2005**, *3*, 503.
11. de Vries, E. F. J.; van Waarde, A.; Buursma, A. R.; Vaalburg, W. *J. Nucl. Med.* **2003**, *44*, 1700.
12. The [^{11}C]methylated analogue of the valdecoxib metabolite **5** has been reported. See: Kumar, J. S. D.; Prabhakaran, J.; Underwood, M. D.; Simpson, N. R.; Parsey, R. V.; Majo, V. J.; Arcement, J.; Arango, V.; van Heertum,

R.; Mann, J. J. Abstract of Papers, 50th Annual Meeting of the Society of Nuclear Medicine, New Orleans, LA; Society of Nuclear Medicine: VA, 2003; Abstract 1110.
13. O'Hagan, D.; Rzepa, H. S. *Chem. Commun.* **1997**, 645.
14. Gierse, J. K.; Hauser, S. D.; Creeley, D. P.; Koboldt, C.; Rangwala, S. H.; Isakson, P. C.; Seibert, K. *Biochem. J.* **1995**, *305*, 479.
15. (a) Reddy, S. T.; Herschman, H. R. *J. Biol. Chem.* **1994**, *269*, 15473; (b) Wadleigh, D. J.; Reddy, S. T.; Kopp, E.; Ghosh, S.; Herschman, H. R. *J. Biol. Chem.* **2000**, *275*, 6259.
16. ^{1}H NMR (360 MHz; CD_3OD, TMS) δ 5.45 (2H, d, $J = 47$ Hz, CH_2F), 7.36–7.48 (7H, m) and 7.89–7.95 (2H, m) (*Ar*). HRMS (EI): calcd for $C_{16}H_{13}FN_2O_3S$ ($[M]^+$) 332.0631, found 332.0624.
17. ^{1}H NMR (360 MHz; CD_3OD, TMS) δ 3.23 (2H, dt, $J = 25$, 5.8 Hz, CH_2CH_2F), 4.74 (2H, dt, $J = 47$, 5.8 Hz, CH_2CH_2F), 7.32–7.44 (7H, m) and 7.89–7.93 (2H, m) (*Ar*). HRMS (EI): calcd for $C_{17}H_{15}FN_2O_3S$ ($[M]^+$) 346.0780, found 346.0780.
18. Talley, J. J.; Brown, D. L.; Carter, J. S.; Graneto, M. J.; Koboldt, C. M.; Masferrer, J. L.; Perkins, W. E.; Roger, R. S.; Shaffer, A. F.; Zhang, Y. Y.; Zweifel, B. S.; Seibeert, K. *J. Med. Chem.* **2000**, *43*, 775.
19. Talley, J. J. U.S. Patent 5,859,257, 1999; *Chem. Abstr.* **1999**, *130,* 110269.
20. Kumar, J. S. D.; Ho, M. M.; Leung, J. M.; Toyokuni, T. *Adv. Synth. Catal.* **2002**, *344*, 1146.
21. ^{1}H NMR (360 MHz; $CDCl_3$, TMS) δ 2.43 (3H, s, Ph*Me*), 3.75 (6H, s, O*Me*), 5.11 (2H, s, CH_2), 5.80 (1H, br s, N*H*), 6.70 (4H, d, $J = 7.2$ Hz), 6.94 (2H, d, $J = 7.2$ Hz), 7.16–7.45 (18H, m) and 7.79 (2H, d, $J = 7.2$ Hz) (Ar). HRMS (FAB): calcd for $C_{44}H_{39}N_2O_8S_2$ ($[M+H]^+$) 787.2148, found 787.2147.
22. ^{1}H NMR (360 MHz; $CDCl_3$, TMS) δ 3.75 (6H, s, O*Me*), 4.75 (2H, s, CH_2), 5.85 (1H, s, N*H*), 6.68 (4H, d, $J = 7.2$ Hz), 7.05 (2H, d, $J = 7.2$ Hz) and 7.15–7.45 (16H, m) (*Ar*). HRMS (EI): calcd for $C_{37}H_{32}N_2O_6S$ ($[M]^+$) 632.1981, found 632.1977.
23. No-carrier-added [^{18}F]fluoride (~500 mCi; specific activity: >10,000 Ci/mmol) was produced by $^{18}O(p,n)^{18}F$ nuclear reaction of 95% [^{18}O]H_2O. The radioactivity (~500 mCi) was transferred to a glass reaction vessel containing azacrown ether Kryptofix 222 (10 mg) and K_2CO_3 (1.0 mg) in MeCN–H_2O (25:1 v/v, 1 mL). After removal of H_2O at 110 °C with a stream of N_2, the residue was dried further by the azeotropic distillation with MeCN (1.0, 0.5 and 0.5 mL). A solution of **8** (5 mg) in MeCN (1 mL) was added and the mixture was heated at 90 °C for 5 min. A 40% solution of trichloroacetic acid in MeCN (0.5 mL) was added and the mixture was kept at 90 °C for an additional 5 min. After partial neutralization with saturated aq $NaHCO_3$ (0.7 mL), the mixture was diluted with H_2O (7.3 mL) and passed through a Waters Sep-Pak C-18 cartridge (1 mL). The cartridge was washed successively with H_2O (4 mL) and with 50 mM aq NH_4OAc (2 × 4 mL). The crude product was subsequently eluted with MeOH (1.8 mL). The MeOH eluate was purified by HPLC (Phenomenex Aqua C-18, 5 μm, 250 × 10 mm) with THF–MeOH–10 mM aq NH_4OAc (20:25:55 v/v/v) at 5 mL/min. The elution was monitored using a UV detector (254 nm) and a γ detector. The chemically and radiochemically pure fraction (~10 mL; t_R ~25 min) was collected, diluted with H_2O (60 mL), and passed through a Waters Sep-Pak C-18 cartridge (1 mL). After washing the cartridge with H_2O (20 mL), the product was eluted with EtOH (1 mL) to a sterile vial through a Millipore Millex-GS filter (0.22 μm) to give **1-^{18}F** as a 1-mL EtOH solution (~80 mCi). The chemical and radiochemical purity, as well as chemical identity, was confirmed using analytical HPLC (Phenomenex Aqua C-18, 5 μm, 250 × 4.6 mm) with MeCN–H_2O (1:1 v/v) containing 0.01% TFA at 1 mL/min by reference to the non-radioactive **1** (t_R ~ 10 min). The radiochemical purity was ascertained further by radio-TLC on silica gel (R_f 0.45; hexanes–EtOAc 1:1 v/v). The total synthesis time was ~120 min from EOB and the decay-corrected radiochemical yield was ~40%. The specific activity was determined to be ~2000 Ci/mmol at EOS based on the UV absorption and concentration standard curve.
24. The product was kept in EtOH until ready for use. For in vivo applications, the solution was diluted with normal saline such that the alcohol concentration was <5%.
25. De[^{18}F]fluorination was monitored by radio-TLC on silica gel, where [^{18}F]fluoride stays at the origin. The non-radioactive **1** was stable in PBS (pH 7.4).
26. A PET scanner for small animals. See: Chatziioannou, A. F. *Eur. J. Nucl. Med. Mol. Imaging* **2002**, *29*, 98.
27. The mouse was anesthetized by xylazine (10 mg/kg) with ketamine (200 mg/kg) and placed in the microPET scanner (Concorde Microsystems Inc., Knoxville, TN). The mouse was then injected via tail vein with **1-^{18}F** (200–300 μCi in 200 μL saline containing <5% EtOH). Dynamic data acquisition commenced in a list mode at the time of injection to obtain a time-dependent organ distribution of radioactivity (frame times and sequence: 10 × 90 s and 21 × 300 s). The data were acquired in a 3-D mode with an axial span of ~8 cm. The images were reconstructed using well-characterized 3-D filtered back-projection methods. The bony skeleton was visible in 15 min post-injection.
28. The monkey, fasted after 9 PM on the evening prior to the PET study, was anesthetized with ketamine (15–20 mg/kg) and maintained anesthetically by inhalant isofluorane techniques (1–2%). The animal was placed supine in the scanner bed. The i.v. injection of **1-^{18}F** (~10 mCi) was followed by the data collection, as described in Ref. 27, except that a series of bed positions was used to cover the entire animal with each position (300-s frames) repeated 3–6 times. The bone structure became visible in 45 min post-injection.
29. (a) Yuan, J. J.; Yang, D.-C.; Zhang, J. Y.; Bible, R., Jr.; Karim, A.; Findlay, J. W. A. *Drug Metab. Dispos.* **2002**, *30*, 1013; (b) Zhang, J. Y.; Yuan, J. J.; Wang, Y.-F.; Bible, R. H., Jr.; Breau, A. P. *Drug Metab. Dispos.* **2003**, *31*, 491–501.
30. Barrio, J. R.; Satyamurthy, N.; Huang, S.-C.; Keen, R. E.; Nissenson, C. H. K.; Hoffman, J. M.; Ackermann, R. F.; Bahn, M. M.; Mazziotta, J. C.; Phelps, M. E. *J. Cerebral Blood Flow Metab.* **1989**, *9*, 830.
31. Stabin, M. G. *J. Nucl. Med.* **1996**, *37*, 538.